HHS Public Access

Author manuscript

Nat Plants. Author manuscript; available in PMC 2018 May 20.

Published in final edited form as:

Nat Plants. ; 3: 17079. doi:10.1038/nplants.2017.79.

Sperm cells are passive cargo of the pollen tube in plant fertilization

Jun Zhang[1,†], **Qingpei Huang**[1,†], **Sheng Zhong**[1,†], **Andrea Bleckmann**[2], **Jiaying Huang**[1], **Xinyang Guo**[1], **Qing Lin**[1], **Hongya Gu**[1,3], **Juan Dong**[4], **Thomas Dresselhaus**[2], and **Li-Jia Qu**[1,3,*]

[1]State Key Laboratory for Protein and Plant Gene Research, Peking-Tsinghua Center for Life Sciences at College of Life Sciences, Peking University, Beijing 100871, China

[2]Cell Biology and Plant Biochemistry, Biochemie-Zentrum Regensburg, University of Regensburg, 93053 Regensburg, Germany

[3]The National Plant Gene Research Center (Beijing), Beijing 100101, China

[4]The Waksman Institute of Microbiology, Rutgers the State University of New Jersey, Piscataway, New Jersey 08854, USA

Abstract

Sperm cells of seed plants have lost their motility and are transported by the vegetative pollen tube cell for fertilization, but the extent to which they regulate their own transportation is a long-standing debate. Here we show that *Arabidopsis* lacking two bHLH transcription factors produces pollen without sperm cells. This abnormal pollen mostly behaves like the wild type and demonstrates that sperm cells are dispensable for normal pollen tube development.

Seed plants have conquered almost every habitat on earth due to the development of special characteristics that are adaptive to new environments, for example, the formation of a vasculature, roots, guard cells and, in particular, specialized reproductive systems to protect gametes and to ensure fertilization success[1]. Male reproductive organs generate pollen grains, which produce pollen tubes, each consisting of a vegetative cell that engulfs two immotile sperm cells[2]. This structure is also known as the male germ unit[3]. Due to the absence of a motility system, sperm cells of flowering plants rely on directional growth of the pollen tube toward the egg apparatus, which is deeply embedded in the maternal tissues

*qulj@pku.edu.cn.

†These authors contributed equally to this work.

Correspondence and requests for materials should be addressed to L.-J.Q.

Author contributions

L.-J.Q., H.G., J.D. and T.D. designed the study; Q.L. generated single mutants. J.Z. and Q.H. generated double mutants and, together with S.Z. and A.B., performed phenotypic analysis. Q.H. and J.Z. conducted RNA-seq analysis; Q.H. and J.H. performed bioinformatics analysis. X.G. and S.Z. performed the SIV PT attraction assay. L.-J.Q., J.Z., S.Z., H.G., J.D. and T.D. interpreted the data and wrote the manuscript.

Supplementary information is available for this paper.

Competing interests

The authors declare no competing financial interests.

of the ovary and ovule, respectively[1]. Once the pollen tube tip recognizes the egg apparatus, it ruptures to release the sperm cells for double fertilization: one sperm cell fuses with the egg cell to initiate embryo development and the other one fuses with the central cell to develop into an endosperm[1]. The whole process of pollination and fertilization in plants requires tightly controlled spatiotemporal cell–cell communication events for robust pollen tube growth and directional guidance[1]. It is assumed that the tube cell plays provocative roles in cell–cell communication[4], but whether and to what extent sperm cells also contribute to these events has been a longstanding debate. Previous research in the model plant *Arabidopsis thaliana* (*Arabidopsis*), for example, has shown that the vegetative nucleus of the male germ unit precedes sperm cells during the journey[5], suggesting a passive feature of sperm cell transport. However, in maize, sperm cell movement is highly dynamic and changes positions during tube growth[6], indicating a more active role. Similarly, in the *Arabidopsis wit12* and *wip123* mutants, sperm cells precede the vegetative nucleus and pollen tube perception appears defective[7]. To ultimately elucidate the extent to which sperm cells contribute to the regulation of the pollen tube journey, mutants that generate pollen tubes lacking sperm cells are required. Here, we report the identification of such a novel mutant and demonstrate a negligible role of the sperm cells in pollen tube growth and male–female communication.

We studied three related basic helix-loop-helix (bHLH) transcription factor genes in *Arabidopsis*, *DEFECTIVE REGION OF POLLEN 1* (*DROP1*, At2g24260), *DROP2* (At4g30980) and *DROP3* (At5g58010) (Fig. 1a), which were previously reported to function in root hair development and called *LRL* (*Lj-RHL1-LIKE*), (ref. 8). RNA sequencing (RNA-seq) data[9] shows that *DROP1* is mostly expressed in seeds and *DROP2* in pollen grains and tubes (Fig. 1a). Single knockout mutants for each gene exhibit normal development (Supplementary Fig. 1a–j) and a typical Mendelian segregation ratio (Supplementary Table 1). However, we could not identify *drop1−/− drop2−/−* double mutants. Reciprocal crosses showed that male transmission of either *drop1+/− drop2−/−* or *drop1−/− drop2+/−* mutants was completely blocked (Supplementary Table 1). The homozygous *drop1−/− drop2−/−* mutations were only detected when either *DROP1* or *DROP2* was transformed to complement the heterozygous plants (Supplementary Fig. 2). Thus, *DROP1* and *DROP2* appear redundantly essential for male transmission in *Arabidopsis*.

Developmental defects in *drop1+/− drop2−/−* mutants occur mainly in pollen mitosis II (Supplementary Fig. 3a–d). Half of mature pollen grains from *drop1+/− drop2−/−* and *drop1−/− drop2+/−* heterozygous plants were unviable and aberrant in morphology. Of these, approximately 40% contained one vegetative-like nucleus lacking condensed sperm cells and approximately 60% did not contain any nucleus (Fig. 1b–e). We next crossed the mutant *quartet1* (*qrt1*) (ref. 10) with both heterozygous mutants for tetrad analysis. In the wild type (WT), all four mature pollen grains of *qrt1* were tri-cellular (Supplementary Fig. 4), whereas in either *drop1+/− drop2−/− qrt1* or *drop1−/− drop2+/− qrt1*, two (50%) of the four mature pollen grains were tri-cellular while the other two showed abnormal shapes, either like a water-drop containing one nucleus or collapsed lacking a nucleus (Fig. 1f–i). Because 50% of pollen grains are expected to be *drop1+ drop2−* or *drop1− drop2+* and looking normal in these mutants, the abnormal pollen grains must be homozygous *drop1−*

drop2−. Notably, the single-nucleated *drop1*− *drop2*− pollen showed aberrant morphology: cell walls were deformed and accompanied by cytoplasmic protrusions (Fig. 1c,j,k).

To clarify the identity of the vegetative-like nucleus in the mutant pollen grains, we crossed *drop1*−/− *drop2*+/− with two double marker lines, *ProLAT52:GFP*/*ProHTR10:HTR10-RFP* (ref. 11) (Fig. 1l) and *ProLAT52:H2B-GFP/ProDUO1:tdTomato* (Fig. 1n), which label the vegetative cell and its nucleus in green and the sperm nuclei in red. In contrast to WT pollen (Fig. 1l,n), mononucleated *drop1*− *drop2*− pollen expressed the vegetative cell markers only (green in Fig. 1m,o). Another vegetative nucleus marker, *ProWIP1::WIP1-tdTomato* (ref. 7), was also detectable in both WT and *drop1*− *drop2*− pollen (Fig. 1p,q). These results clearly demonstrate the identity of the single vegetative nucleus in *drop1*− *drop2*− pollen and further support the finding that defective *drop1*− *drop2*− pollen lacks sperm cells.

Morphologically aberrant *drop1*− *drop2*− pollen grains were manually picked under a light microscope (single vegetative nucleus confirmed by 4,6-diamidino-2-phenylindole (DAPI) staining) (Supplementary Fig. 5) and used for RNA-seq analysis after pollinated and grew through the stigma/style (semi-*in vivo* pollen tubes (SIV PTs)). As shown in Fig. 1r, neither *DROP1* nor *DROP2* was expressed in mutant SIV PTs, confirming the feasibility of the manually picked *drop1*− *drop2*− pollen. The expression of vegetative cell-specific genes such as *WIP1* (ref. 7) and *UBQ10* (ref. 12) in *drop1*− *drop2*− was comparable or even higher compared to WT. However, the expression of sperm cell-specific genes including *DUO1* (ref. 13), *GCS1/HAP2* (ref. 13), *DAU2* (ref. 13), *DAA1* (ref. 13) and *OPT8* (ref. 18) was almost completely absent (Fig. 1r), explicitly supporting that *drop1*− *drop2*− pollen tubes lack sperm cells.

This discovery allowed us to study the regulatory role of the pollen tube cell during the entire journey toward the ovule. We found that, similar to the WT (Fig. 2a,b), *drop1*− *drop2*− pollen grains (Fig. 2c,d) germinated *in vitro*, although at a lower rate (Fig. 2e). Similarly, *drop1*− *drop2*− pollen grains germinate *in vivo* and pollen tubes penetrate female tissues successfully and grow at a comparable speed as WT tubes (Fig. 2f–h). These results suggest that *drop1*− *drop2*− pollen grains are capable of germinating and the tubes can grow and respond to female signals during early stages of the pathway.

Moreover, mutant pollen tubes could successfully target the micropylar entrance of WT ovules *in vivo* (Supplementary Fig. 6a,b). An ovule targeting assay[14] revealed that 100% of mutant SIV PTs efficiently oriented their growth direction towards ovules and reached the micropyle successfully (Supplementary Fig. 6c–f). An SIV PT attraction assay using recombinant LURE1.2 polypeptide, an ovule-secreted attractant[4], showed that, similar to the WT (95%, $n = 15$; Fig. 2i–k), almost all mutant SIV PTs (92%, $n = 12$) turned sharply toward LURE1-embedded beads within minutes (Fig. 2l–n). This observation unambiguously demonstrated that mutant pollen tubes maintained normal responsiveness to female attraction cues.

When pollen tubes enter the ovule, they rupture to release sperm cells for double fertilization. We found that both WT (Fig. 2o,p) and *drop1*− *drop2*− pollen tubes (Fig. 2q,r) underwent rupture after entering the ovule. Moreover, the expressions of known genes

involved in pollen tube growth and guidance (for example, *LIP1/2* (ref. 4), *COBL10* (ref. 15), *MPK3/6* (ref. 15), *CHX21/23* (ref. 15), *MDIS1/2* (ref. 15) and *PRK1/6/3/8* (ref. 15)) and in pollen tube rupture (for example, *MYB97/101/120* (ref. 11) and *ANX1/2* (ref. 16)) were detected in *drop1− drop2−* SIV PTs (Supplementary Fig. 7). Thirty-six hours after pollination (HAP), while developing embryo and endosperm were evident in WT ovules (Fig. 2s), however, embryo and endosperm development was absent in *drop1− drop2−* pollen tube-targeted ovules (Fig. 2t), consistent with the fact that sperm cells were absent in mutant pollen tubes.

In conclusion, *Arabidopsis drop1−/− drop2−/−* represents a novel male gametophytic mutant that produces a functional pollen tube lacking sperm cells. The absence of sperm cells distinguishes this novel mutant from other known mutants, such as *duo1* (ref. 13), *duo3* (ref. 13), *daz1* (ref. 17), *daz2* (ref. 17) and *cdka1* (ref. 18), in which generative or sperm cells are still present. Taking advantage of this unique mutant, we demonstrate that the vegetative pollen tube cell is sufficient to regulate the entire journey and serves as an active vehicle to navigate and deliver sperm cells, as a passive cargo, into the ovule for double fertilization. Future studies are required to understand the role of DROP1/2 for germ cell fate determination and differentiation in flowering plants.

Methods

Plant material and growth conditions

A. thaliana ecotype Columbia-0 (Col-0) was used as the WT. All transgenic plants in this study were in the Col-0 background. The *drop1* mutant (Salk_006430), *drop2* mutant (Salk_029317) and *drop3* mutant (Salk_015021) were obtained from the *Arabidopsis* Biological Resource Center. Plants were grown in the greenhouse with LED lights (GPL production modules DR/W and DR/B/FR, Philips) under long-day conditions (16 h light/8 h dark) at 22 °C.

Genotyping analysis

The genotype of *drop1* was confirmed by primers DROP1-rp/DROP1-lp and DROP1-rp/LBb1.3 (T-DNA primer, http://signal.salk.edu/tdnaprimers.2.html). The genotype of *drop2* was confirmed by primers DROP2-rp/DROP2-lp and DROP2-rp/LBb1.3 (Supplementary Table 2). *drop3* was investigated as described previously[8]. The insertion site was confirmed by sequencing. The genotype of *drop1* and *drop2* with transformed constructs was confirmed by primers DROP1-rp/DROP1-lp2 and DROP2-rp/DROP2-lp2, respectively (Supplementary Table 2).

Aniline blue staining

For aniline blue staining, stamens of floral stage 12 flowers were emasculated. At 12–24 h later, about 30–40 pollen grains from WT or mutant plants were dispersed onto stigma papilla cells. Abnormal-looking *drop1− drop2−* mutant pollen grains were manually isolated with an eyelash pen under a stereoscopic microscope (Optec SZ650). Such pollen grains were stained with DAPI to further confirm their nuclear status under a fluorescence microscope (Olympus BX51). To visualize pollen tube growth, pollinated pistils were

excised and fixed in FAA solution (acetic acid/EtOH (1:3) solution) for more than 24 h, followed by rehydration through a graded ethanol series of 70, 50, 30% and ddH_2O. Samples were further softened with 8 M NaOH overnight at room temperature and then washed three times with water. Pollen tubes were then stained by 0.1% decolorized aniline blue (pH = 9–11, in 108 mM K_3PO_4) for more than two hours in the dark. Stained samples were observed under a fluorescence microscope (Olympus BX51) equipped with a UV filter set.

In vitro pollen germination analysis

Pollen grains from freshly opened flowers were dispersed onto solid pollen germination medium (SPGM) (18% sucrose, 0.01% boric acid, 2 mM $CaCl_2$, 1 mM $Ca(NO_3)_2$, 1 mM KCl, 1 mM $MgSO_4$, adjusted to pH = 7, 1.5% agar) and incubated in a humid box for germination at 22 °C for 5–6 h. Pollen tube length and germination rate were measured and calculated by Image J software (National Institutes of Health, http://rsbweb.nih.gov/ij/).

SIV PT attraction assay

SPGM contained 10% sucrose, 0.01% boric acid, 5 mM $CaCl_2$, 5 mM KCl, 1 mM $MgSO_4$ and was adjusted to pH = 7.5 before adding low melting-agarose to a final concentration of 1.5%. For the semi-*in vivo* attraction assay, hand-cut styles of *ms1* mutant plants[19] were placed on the SPGM in a small culture dish with a 2-mm-thick cover glass in the bottom centre. After the detached styles were pollinated, the culture dish was placed into a 22 °C incubator. The insect cell-produced peptides (AtLURE1.2) were used for the pollen tube attraction assay. The following semi-*in vivo* attraction steps were conducted according to previously reported protocols[15].

Confocal microscopy

Fluorescence images were observed and collected on a Zeiss spinning disk confocal microscope equipped with a Yokogawa CSU-X1 spinning disk and an evolve charge-coupled device camera with a 20× air objective lens and a 40× water objective lens. A 20× air objective lens was used for semi-*in vivo* attraction images under 405 nm, 488 nm and bright-field illumination. A 40× water objective lens was used for marker line labelling observation, under 488 nm and 532 nm.

Differential interference contrast observation

To examine embryogenesis in ovules, siliques were fixed with a 3:1 mixture of ethanol and acetic acid (v/v) 36 HAP. Samples were rehydrated with an ethanol series and cleared in a mixture of 7.5 grams of gum arabic, 80 grams of chloral hydrate, 8 ml of glycerol and 30 ml of H_2O. Cleared samples were viewed with differential interference contrast microscopy (AxioImager D2, Zeiss).

RNA sequencing and RNA-seq data analysis

About 500–600 double mutant *drop1 drop2* pollen grains were hand-picked under a stereoscopic microscope and pollinated on a single stigma (emasculated for 36 h) and cut together with the style. When the SIV PTs grew about 300–400 μm outside of the style, they

were cut from the end of the style with tiny scissors (VANNAS, 8.5 cm, STR) under a stereo microscope. Pollen tubes cut from two independent stigmas were pooled and directly placed into cell lysis buffer (0.45 μl 10×PCR buffer II, 0.27 μl 25 mM$MgCl_2$, 0.225 μl 10% NP40, 0.225 μl 0.1 M DTT, 0.045 μl SUPERase-In (20 U per μl, Ambion), 0.045 μl RNase inhibitor (40 U per μl, Ambion), 0.125 μl 0.5 μM V1-T24 primer, 0.09 μl 2.5 mM dNTP mix, add H_2O to 4.45 μl) and lysed by vortexing. The lysed solution was used to generate the cDNA libraries following the Smart-seq2 protocol designed for single cells[20]. The RNA-seq analysis of *drop1 drop2* pollen grains has been conducted only once due to the extreme difficulty to obtain this material. Read length generated by an Illumina HiSeq 4000 sequencer was 150 bp of pair-end sequencing. Tophat (version 2.0.14) was used to map the *A. thaliana* genome of TAIR10 version (parameters: -i 36 -I 20000 -p 5 -r 20 –mate-std-dev 50). Cufflinks (version 2.2.1) was used to normalize and verify expression level of the two samples (parameters: default)[21].

Data availability

The RNA-seq data are deposited to Gene Expression Omnibus with the accession number GSE98145.

Supplementary Material

Refer to Web version on PubMed Central for supplementary material.

Acknowledgments

We thank F. Tang and Y. Hu (Peking University, China) for technical help in single-cell RNA extraction, library construction and RNA-seq analysis. We are grateful to T. Aoyama and T. Tsuge (Kyoto University, Japan) for suggestions on preparing the manuscript. This work is supported by National Natural Science Foundation of China (grant Nos. 31620103903, 31621001 and 31370344) and partially by the 111 project. The Qu laboratory is supported by the Peking-Tsinghua Joint Center for Life Sciences and the Dresselhaus lab by the Collaborative Research Center SFB924. The supplementary materials contain additional data.

References

1. Dresselhaus T, Sprunck S, Wessel GM. Curr Biol. 2016; 26:R125–R139. [PubMed: 26859271]
2. McCue AD, Cresti M, Feijo JA, Slotkin RK. J Exp Bot. 2011; 62:1621–1631. [PubMed: 21357775]
3. Dumas C, Knox RB, Gaude T. Protoplasma. 1985; 124:168–174.
4. Liu J, et al. Curr Biol. 2013; 23:993–998. [PubMed: 23684977]
5. Hamamura Y, et al. Curr Biol. 2011; 21:497–502. [PubMed: 21396821]
6. Kliwer I, Dresselhaus T. Plant Signal Behav. 2010; 5:885–889. [PubMed: 20505353]
7. Zhou X, Meier I. Proc Natl Acad Sci USA. 2014; 111:11900–11905. [PubMed: 25074908]
8. Lin Q, et al. Plant Cell. 2015; 27:2894–2906. [PubMed: 26486447]
9. Huang Q, Dresselhaus T, Gu H, Qu LJ. J Integr Plant Biol. 2015; 57:518–521. [PubMed: 25828584]
10. Preuss D, Rhee SY, Davis RW. Science. 1994; 264:1458–1460. [PubMed: 8197459]
11. Leydon AR, et al. Curr Biol. 2013; 23:1209–1214. [PubMed: 23791732]
12. Schönberger J, Hammes UZ, Dresselhaus T. Plant J. 2012; 71:173–181. [PubMed: 22268772]
13. Berger F, Twell D. Annu Rev Plant Biol. 2011; 62:461–484. [PubMed: 21332359]
14. Hou Y, et al. Curr Biol. 2016; 26:2343–2350. [PubMed: 27524487]
15. Higashiyama T, Yang W. Plant Physiol. 2017; 173:112–121. [PubMed: 27920159]
16. Boisson-Dernier A, et al. Development. 2009; 136:3279–3288. [PubMed: 19736323]

17. Borg M, et al. Plant Cell. 2014; 26:2098–2113. [PubMed: 24876252]
18. Iwakawa H, Shinmyo A, Sekine M. Plant J. 2006; 45:819–831. [PubMed: 16460514]
19. Yang CY, Vizcay-Barrena G, Conner K, Wilson Z. Plant Cell. 2007; 19:3530–3548. [PubMed: 18032629]
20. Picelli S, et al. Nat Methods. 2013; 10:1096–1098. [PubMed: 24056875]
21. Trapnell C, et al. Nat Protoc. 2012; 7:562–578. [PubMed: 22383036]

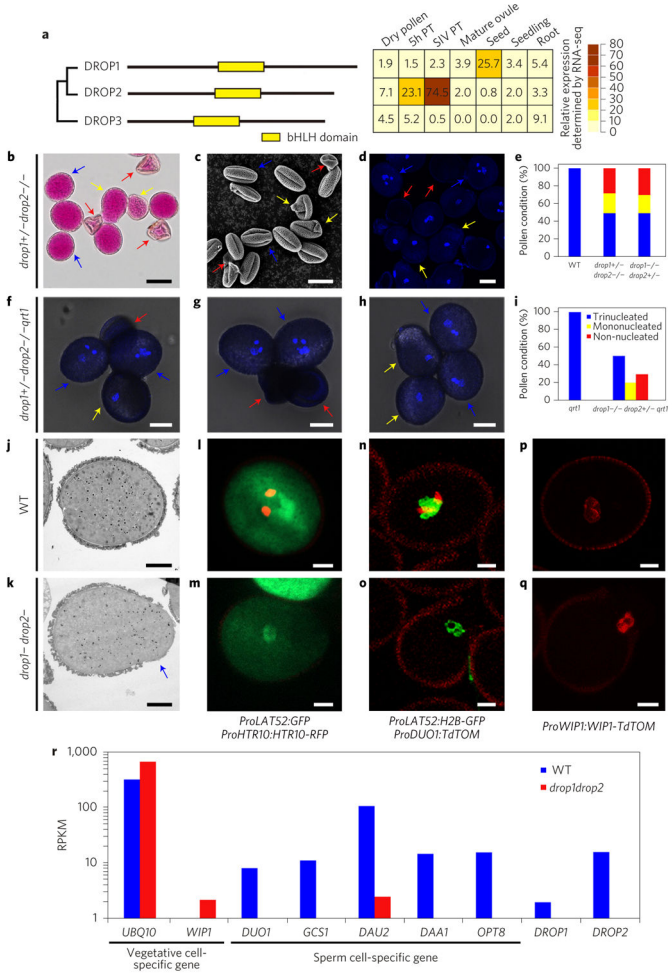

Figure 1. The *drop1− drop2−* pollen grains lack sperm cells

a, Left: phylogenic tree shows the relationship of three DROP proteins. The conserved bHLH domain is indicated by a yellow box. Right: heatmap indicating the relative expression level of each *DROP* gene in different tissues. Values were taken from RNA-seq data using designated tissues. **b**–**d**, Alexander's staining (**b**), scanning electron microscopy (**c**) and DAPI-staining (**d**) of *drop1+/− drop2−/−* pollen. Blue arrows indicate WT-looking pollen; yellow arrows indicate water drop-like pollen; red arrows indicate collapsed pollen. **e**, Statistical analysis of pollen defects in *drop* mutants as indicated. **f**–**h**, Bright-field-UV merged images of mature pollen grains of *drop1−/− drop2+/− qrt1* mutant. **i**, Statistical analysis of pollen defects in *drop1−/− drop2+/− qrt1*. **j**,**k**, Transmission electron microscopy of WT and *drop1− drop2−* pollen, respectively. Blue arrow indicates abnormal cytoplasmic protrusion. **l**–**q**, Confocal laser scanning microscopy of WT and *drop1− drop2−* pollen expressing different reporters. The vegetative marker *ProLAT52:GFP* is present in both WT (green in **l**) and *drop1− drop2−* mutants (**m**), but the generative cell marker *ProHTR10:HTR10-RFP* (red in **l**) is absent from *drop1− drop2−* pollen (**m**). In **n** and **o**, expression of the double marker line *ProLAT52:H2B-GFP* (green, vegetative nucleus) *ProDUO1:TdTOM* (red, generative cell) in WT and *drop1− drop2−* pollen, respectively. In **p** and **q**, the vegetative marker *ProWIP1:WIP1-TdTOM* (red) is expressed in both WT and

drop1− drop2− pollen*,* respectively. **r**, Quantification of expression levels of vegetative and sperm cell-specific genes in semi-*in vivo* grown WT (blue bars) and in *drop1− drop2−* (red bars) pollen tubes. PT, pollen tube; RPKM, reads per kilobase per million reads. Scale bars, 20 μm (**b**); 10 μm (**c**,**d**,**f**,**g**,**h**); 5 μm (**j**–**q**).

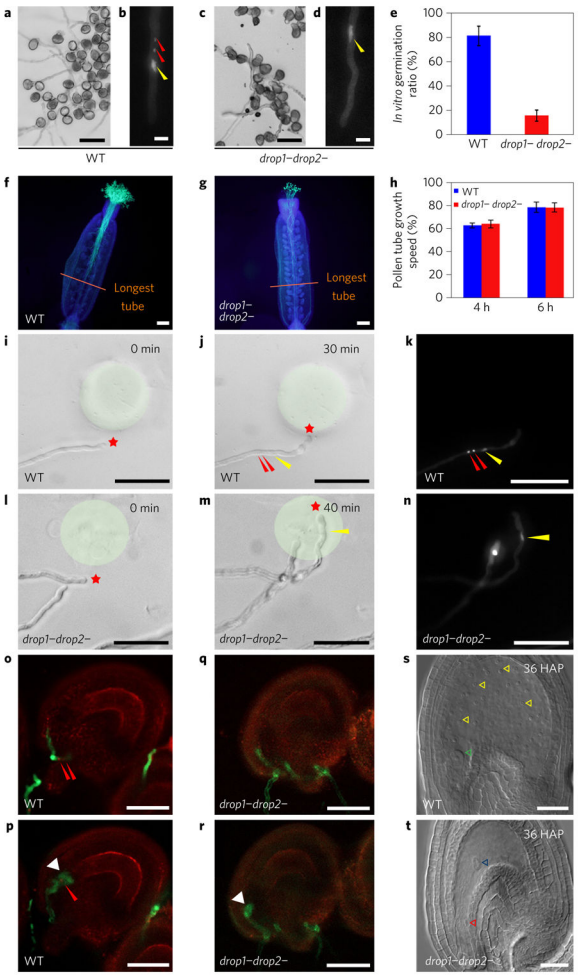

Figure 2. Sperm-less *drop1− drop2−* mutant pollen tubes grow normally toward the ovule

a–**d**, *In vitro* germination and growth of WT (**a**,**b**) and *drop1− drop2−* pollen (**c**,**d**). Panels **a** and **c** show bright-field microscopy images; **b** and **d** show epifluorescence microscopy of DAPI-stained pollen tubes. Yellow arrowhead points to the vegetative nucleus; red arrowhead indicates the sperm cell nucleus. **e**, Statistical analysis of *in vitro* germination ratio of WT and *drop1− drop2−* pollen. **f**,**g**, Aniline blue staining of emasculated WT pistil that was pollinated with WT pollen (**f**) and *drop1− drop2−* pollen (**g**) 4HAP, respectively. The orange line marks the furthest point of pollen tube growth. Note that pollen tubes of *drop1− drop2−*, similar to those of WT, reach the end of the pistil. **h**, Statistical analysis of the growth speed of *in vivo* pollen tubes in pistils 4 HAP and 6 HAP. **i**–**n**, SIV PT attraction assay tracing guided pollen tube growth towards recombinant attraction protein AtLURE1.2 in a gelatin bead (shaded with light green). Asterisk indicates the tip of a growing pollen tube at different points. The identity of nuclei in **j**,**m** was revealed by DAPI staining (**k**,**n**, respectively). Red arrowhead marks the sperm cell nucleus; yellow arrowhead indicates the vegetative nucleus. **o**–**t**, WT and *drop1− drop2−* pollen tube targeting (**o** for WT and **q** for the mutant) and rupture (**p** for WT and **r** for the mutant). In **s**, seed development is initiated from WT ovules (yellow arrowheads indicate endosperm nuclei, and green arrow head the embryo), but not after the rupture of *drop1− drop2−* pollen tubes. In **t**, the blue arrowhead

indicates the central cell and the red arrowhead indicates the egg cell. In **e** and **h**, data and error bars represent the mean ± s.d. Scale bars, 20 μm (**a**,**c**,**s**,**t**); 10 μm (**b**,**d**); 200 μm (**f**,**g**); 100 μm (**i**–**n**); 50 μm (**o**–**r**).